Inorg. Chem. **2005**, *44*, 2513–2523

Mononuclear and Dinuclear Complexes of Isoeilatin

Sheba D. Bergman,[†] Israel Goldberg,[†] Andrea Barbieri,[‡] and Moshe Kol*[,†]

The School of Chemistry, Raymond and Beverly Sackler Faculty of Exact Sciences, Tel Aviv University, Tel Aviv 69978, Israel, and Istituto per la Sintesi Organica e la Fotoreattività, Consiglio Nazionale delle Ricerche (ISOF-CNR), Via P. Gobetti 101, 40129 Bologna, Italy

Received January 2, 2005

This work describes the synthesis and characterization of mononuclear and dinuclear Ru(II) and Os(II) complexes based on the symmetrical bridging ligand isoeilatin (**1**). The crystal structure of **1**·$[HCl]_2$ consists of layers of tightly π-stacked molecules of the biprotonated isoeilatin. The mononuclear complexes $[Ru(bpy)_2(ieil)]^{2+}$ ($\mathbf{2}^{2+}$) and $[Os(bpy)_2(ieil)]^{2+}$ ($\mathbf{3}^{2+}$) form discrete dimers in solution held together by face-selective π-stacking interactions via the isoeilatin ligand. Coordination of a second metal fragment does not hinder the π-stacking completely, as demonstrated by the concentration dependence of the ^{1}H NMR spectra of the dinuclear complexes $[\{Ru(bpy)_2\}_2\{\mu\text{-ieil}\}]^{4+}$ ($\mathbf{4}^{4+}$), $[\{Os(bpy)_2\}_2\{\mu\text{-ieil}\}]^{4+}$ ($\mathbf{5}^{4+}$), and $[\{Ru(bpy)_2\}\{\mu\text{-ieil}\}\{Os(bpy)_2\}]^{4+}$ ($\mathbf{6}^{4+}$) and supported by the solid-state structure of *meso*-**4**·$[Cl]_4$. The bridging isoeilatin ligand conserves its planarity even upon coordination of a second metal fragment, as demonstrated in the solid-state structures of *meso*-**4**·$[Cl]_4$, *meso*-**4**·$[PF_6]_4$, and *meso*-**5**·$[PF_6]_4$. All of the dinuclear complexes exhibit a preference (3/2–3/1) for the formation of the heterochiral as opposed to the homochiral diastereoisomer. Absorption spectra of the mononuclear complexes feature a low-lying $d_\pi(M) \rightarrow \pi^*$-(ieil) MLCT band around 600 nm that shifts to beyond 700 nm upon coordination of a second metal fragment. Cyclic and square-wave voltammetry measurements of the complexes exhibit two isoeilatin-based reduction waves that are substantially anodically shifted compared to $[M(bpy)_3]^{2+}$ (M = Ru, Os). Luminescence spectra, quantum yields, and lifetime measurements at room temperature and at 77 K demonstrate that the complexes exhibit ^{3}MLCT emission that occurs in the IR region between 950 and 1300 nm. Both the electrochemical and photophysical data are consistent with the low-lying π^* orbital of the isoeilatin ligand. The dinuclear complexes exhibit two reversible, well-resolved, metal-centered oxidation waves, despite the chemical equivalence of the two metal centers, indicating a significant metal–metal interaction mediated by the bridging isoeilatin ligand.

Introduction

Over the past several years, molecular architectures consisting of Ru(II) and Os(II) polypyridyl complexes connected by bridging ligands have been studied rigorously.[1,2] The structure, rigidity, and electronic character of the bridging ligands bound to the metal centers determine the energy and intensity of the metal-to-ligand charge-transfer (MLCT) transitions; the lifetime of the excited states; the stability of the oxidized and reduced forms of these complexes; and most importantly, the extent of electronic communication between the metal centers.[3,4] Extended fused aromatic ligands (e.g., tpphz[5] and its analogues,[6] HAT,[7] and ppz[8]) have attracted considerable attention because of their highly delocalized nature, leading to lower-lying MLCT transitions, longer excited state lifetimes, and anodically shifted reduction potentials. In addition, the large π-surface of such ligands facilitates nucleic acid intercalation,[9] as well as mediation of energy and electron transfer.[10] Bridging ligands bearing 2,2′-biquinoline-type (biq) or 2-(2′-pyridyl)-quinoline-type (pq) coordination sites are particularly interesting,[11,12] because the steric crowding introduced by the additional benzo rings markedly changes the metal chelating

* To whom correspondence should be addressed. E-mail: moshekol@post.tau.ac.il.
† Tel Aviv University.
‡ Consiglio Nazionale delle Ricerche (ISOF-CNR).

(1) (a) Balzani, V.; Juris, A.; Venturi, M.; Campagna, S.; Serroni, S. *Chem. Rev.* **1996**, *96*, 759. (b) Belser, B.; Bernhard, S.; Blum, C.; Beyeler, A.; De Cola, L.; Balzani, V. *Coord. Chem. Rev.* **1999**, *190*−*192*, 155. (c) Keene, F. R. *Chem. Soc. Rev.* **1998**, *27*, 185. (d) De Cola, L.; Belser, B. *Coord. Chem. Rev.* **1998**, *177*, 301. (e) Beyeler, A.; Belser, B. *Coord. Chem. Rev.* **2002**, *230*, 29. (f) Ward, M. D.; Barigelletti, F. *Coord. Chem. Rev.* **2001**, *216*−*217*, 127. (g) Balzani, V.; Campagna, S.; Denti, G.; Juris, A.; Serroni, S.; Venturi, M. *Acc. Chem. Res.* **1998**, *31*, 26.

10.1021/ic050002q CCC: $30.25
Published on Web 03/08/2005

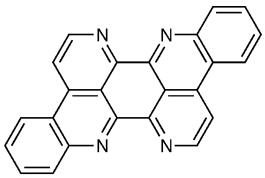

1

Figure 1. Molecular structure of the symmetrical bridging ligand isoeilatin (**1**).

properties[13] and the larger π-surface of these ligands can lead to altered photophysical and electrochemical properties.[14]

Isoeilatin (**1**, Figure 1), a skeletal isomer of the related eilatin ligand,[15] consists of seven fused-aromatic rings arranged in a parallelogram, leading to two identical pq-type coordination sites. In a preliminary communication, we reported that the mononuclear isoeilatin complex $[Ru(bpy)_2(ieil)][PF_6]_2$ (**2**·$[PF_6]_2$) (ieil = isoeilatin) exhibits several unique features:[16] unexpectedly weak yet *face-selective* dimerization in solution induced by $\pi-\pi$ stacking interactions via the isoeilatin moiety; a broad, low-lying metal-to-ligand charge-transfer (MLCT) absorption band; and an anodically shifted reduction of the isoeilatin moiety. In the present study, we set forth to explore the potential of **1** as a bridging ligand and to study the properties of its resulting dinuclear complexes. Specifically, we addressed the following topics: the structural effects of pq-type coordination sites on metal binding; the diastereoisomeric preference in formation of dinuclear species; the effect of binding a second metal fragment on the photophysical and electrochemical properties; the extent of communication between the two metal centers enabled by the isoeilatin bridge, compared to that observed for the related dibenzoeilatin complexes;[11b,11c] and the nature of the excited state. We thus report the synthesis, NMR characterization, crystal structures, electrochemical behavior and photophysical properties of the mononuclear complexes $[Ru(bpy)_2(ieil)]^{2+}$ (**2**$^{2+}$) and $[Os(bpy)_2(ieil)]^{2+}$ (**3**$^{2+}$), the homodinuclear complexes $[\{Ru(bpy)_2\}_2\{\mu\text{-ieil}\}]^{4+}$ (**4**$^{4+}$) and $[\{Os(bpy)_2\}_2\{\mu\text{-ieil}\}]^{4+}$ (**5**$^{4+}$), and the heterodinuclear complex $[\{Ru(bpy)_2\}\{\mu\text{-ieil}\}\{Os(bpy)_2\}]^{4+}$ (**6**$^{4+}$).

Experimental Section

Materials. *rac,cis*-$[Os(bpy)_2Cl_2]$[17] and *rac*-$[Ru(bpy)_2(ieil)][PF_6]_2$ (**2**)[16] were synthesized according to the literature procedures. Tetra-*n*-butylammonium hexafluorophosphate (98%) and silver nitrate

(2) For several recent examples, see: (a) Majumdar, P.; Peng, S.-M.; Goswami, S. *J. Chem. Soc., Dalton Trans.* **1998**, 1569. (b) Zou, X.-H.; Ye, B.-H.; Li, H.; Liu, J.-G.; Xiong, Y.; Ji, L.-N. *J. Chem. Soc., Dalton Trans.* **1999**, 1423. (c) Chao, H.; Li, R.-H.; Jiang, C.-W.; Li, H.; Ji, L.-N.; Li, X.-Y. *J. Chem. Soc., Dalton Trans.* **2001**, 1920. (d) Sommovigo, M.; Denti, G.; Serroni, S.; Campagna, S.; Mingazzini, C.; Mariotti, C.; Juris, A. *Inorg. Chem.* **2001**, *40*, 3318. (e) Richardson, C.; Steel, P. J.; D'Alessandro, D. M.; Junk, P. C.; Keene, F. R. *J. Chem. Soc., Dalton Trans.* **2002**, 2775. (f) Baitalik, S.; Flörke, U.; Nag, K. *J. Chem. Soc., Dalton Trans.* **1999**, 719. (g) Hage, R.; Lempers, H. E. B.; Haasnoot, J. G.; Reedijk, J.; Weldon, F. M.; Vos, J. G. *Inorg. Chem.* **1997**, *36*, 3139. (h) Wang, Y.; Perez, W. J.; Zheng, G. Y.; Rillema, D. P.; Huber, C. L. *Inorg. Chem.* **1998**, *37*, 2227. (i) Otsuki, J.; Omokawa, N.; Yoshiba, K.; Yoshikawa, I.; Akasaka, T.; Suenobu, T.; Takido, T.; Araki, K.; Fukuzumi, S. *Inorg. Chem.* **2003**, *42*, 3057. (j) Kim, M.-J.; Konduri, R.; Ye, H.; MacDonnell, F. M.; Puntoriero, F.; Serroni, S.; Campagna, S.; Holder, T.; Kinsel, G.; Rajeshwar, K. *Inorg. Chem.* **2001**, *41*, 2471. (k) Schlicke, B.; Belser, P.; De Cola, L.; Sabbioni, E.; Balzani, V. *J. Am. Chem. Soc.* **1999**, *121*, 4207. (l) Juris, A.; Prodi, L.; Harriman, A.; Ziessel, R.; Hissler, M.; El-ghayoury, A.; Wu, F.; Riesgo, E. C.; Thummel, R. P. *Inorg. Chem.* **2000**, *39*, 3590. (m) Bilakhiya, A. K.; Tyagi, B.; Paul, P.; Natarajan, P. *Inorg. Chem.* **2002**, *41*, 3830.

(3) (a) Juris, A.; Balzani, V.; Barigelletti, F.; Campagna, S.; Belser, P.; Von Zelewsky, A. *Coord. Chem. Rev.* **1988**, *84*, 85. (b) Balzani, V.; Scandola, F. *Supramolecular Photochemistry*; Ellis Horwood: Chichester, U.K., 1991. (c) Sauvage, J.-P.; Collin, J.-P.; Chambron, J.-C.; Guillerez, S.; Coudret, C.; Balzani, V.; Barigelletti, F.; De Cola, L.; Flamigni, L. *Chem. Rev.* **1994**, *94*, 993.

(4) (a) MacConnell, H. M. *J. Chem. Phys.* **1961**, *35*, 508. (b) Newton, M. D. *Chem. Rev.* **1991**, *91*, 767. (c) Giuffrida, G.; Campagna, S. *Coord. Chem. Rev.* **1994**, *135/136*, 517.

(5) See, for example: (a) Bolger, J.; Gourdon, A.; Ishow, E.; Launay, J.-P. *J. Chem. Soc., Chem. Commun.* **1995**, 1799. (b) Bolger, J.; Gourdon, A.; Ishow, E.; Launay, J.-P. *Inorg. Chem.* **1996**, *35*, 2937. (c) Bodige, S.; Torres, A. S.; Maloney, D. J.; Tate, D.; Kinsel, G. R.; Walker, A. K.; MacDonnell, F. M. *J. Am. Chem. Soc.* **1997**, *119*, 10364. (d) Chiorboli, C.; Bignozzi, C. A.; Scandola, F.; Ishow, E.; Gourdon, A.; Launay, J.-P. *Inorg. Chem.* **1999**, *38*, 2402. (e) Campagna, S.; Serroni, S.; Bodige, S.; MacDonnell, F. M. *Inorg. Chem.* **1999**, *38*, 692. (f) Kim, M.-J.; MacDonnell, F. M.; Gimon-Kinsel, M. E.; Du Bois, T.; Asgharian, N.; Griener, J. C. *Angew. Chem., Int. Ed.* **2000**, *39*, 615.

(6) See, for example: (a) Komatsuzaki, N.; Katoh, R.; Himeda, Y.; Sugihara, H.; Arakawa, H.; Kasuga, K. *J. Chem. Soc., Dalton Trans.* **2000**, 3053. (b) Ishow, E.; Gourdon, A.; Launay, J.-P. *Chem. Commun.* **1998**, 1909. (c) Ishow, E.; Gourdon, A.; Launay, J.-P.; Chiorboli, C.; Scandola, F.; *Inorg. Chem.* **1999**, *38*, 1504. (d) Wärnmark, K.; Heyke, O.; Thomas, J. A.; Lehn, J.-M. *Chem. Commun.* **1996**, 2603. (e) MacDonnell, F. M.; Kim, M.-J.; Wouters, K. L.; Konduri, R. *Coord. Chem. Rev.* **2003**, *242*, 47 and references therein.

(7) See, for example: (a) Masschelein, A.; Kirsch-De Mesmaeker, A.; Verhoeven, C.; Nasielski-Hinkens, R. *Inorg. Chim. Acta* **1987**, *129*, L13. (b) Rutherford, T. J.; Keene, F. R. *Inorg. Chem.* **1997**, *36*, 3580. (c) Rutherford, T. J.; Van Gijte, O.; Kirsch-De Mesmaeker, A.; Keene, F. R. *Inorg. Chem.* **1997**, *36*, 4465. (d) Brodkorb, A.; Kirsch-De Mesmaeker, A.; Rutherford, T. J.; Keene, F. R. *Eur. J. Inorg. Chem.* **2001**, 2151. (e) Rutherford, T. J.; Keene, F. R. *J. Chem. Soc., Dalton Trans.* **1998**, 1155. (f) Moucheron, C.; Kirsch De-Mesmaeker, A. *J. Am. Chem. Soc.* **1996**, *118*, 12834.

(8) See, for example: (a) Fuchs, Y.; Lofters, S.; Dieter, T.; Shi, W.; Morgan, R.; Strekas, T. C.; Gafney, H. D.; Baker, A. D. *J. Am. Chem. Soc.* **1987**, *109*, 2691. (b) Morgan, O.; Wang, S.; Bae, S.-A.; Morgan, R. J.; Baker, A. D.; Strekas, T. C.; Engel, R. *J. Chem. Soc., Dalton Trans.* **1997**, 3773.

(9) (a) Erkkila, K. E.; Odom, D. T.; Barton, J. K. *Chem. Rev.* **1999**, *99*, 2777. (b) Dupureur, C. M.; Barton, J. K. *Inorg. Chem.* **1997**, *36*, 33. (c) Holmlin, R. E.; Yao, J. A.; Barton, J. K. *Inorg. Chem.* **1999**, *38*, 174. (d) Greguric, A.; Greguric, I. D.; Hambley, T. W.; Aldrich-Wright, J. R.; Collins, J. G. *J. Chem. Soc., Dalton Trans.* **2002**, 849. (e) Morgan, R. J.; Chatterjee, S.; Baker, A. D.; Strekas, T. C. *Inorg. Chem.* **1991**, *30*, 2687. (f) Brodkorb, A.; Kirsch-De Mesmaeker, A.; Rutherford, T. J.; Keene, F. R. *Eur. J. Inorg. Chem.* **2001**, 2151.

(10) See, for example: (a) Chiorboli, C.; Rodgers, M. A. J.; Scandola, F. *J. Am. Chem. Soc.* **2003**, *125*, 483. (b) Kim, M.-J.; Konduri, R.; Ye, H.; MacDonnell, F. M.; Puntoriero, F.; Serroni, S.; Campagna, S.; Holder, T.; Kinsel, G.; Rajeshwar, K. *Inorg. Chem.* **2002**, *41*, 2471. (c) Campagna, S.; Serroni, S.; Bodige, S.; MacDonnell, F. M. *Inorg. Chem.* **1999**, *38*, 692. (d) Konduri, R.; Ye, H.; MacDonnell, F. M.; Serroni, S.; Campagna, S.; Rajeshwar, K. *Angew. Chem., Int. Ed.* **2002**, *41*, 3185.

(11) For biq-type ligands, see: (a) Bergman, S. D.; Reshef, D.; Groysman, S.; Goldberg, I.; Kol, M. *Chem. Commun.* **2002**, 2374. (b) Bergman, S. D.; Goldberg, I.; Barbieri, A.; Barigelletti, F.; Kol, M. *Inorg. Chem.* **2004**, *43*, 2355. (c) Bu, X.-H.; Biradha, K.; Yamaguchi, T.; Nishimura, M.; Ito, T.; Tanaka, K.; Shionoya, M. *Chem. Commun.* **2000**, 1953. (d) Kitagawa, S.; Masaoka, S. *Coord. Chem. Rev.* **2003**, *246*, 73.

(12) For pq-type ligands, see: (a) Ruminski, R. R.; Serveiss, D.; Jacquez, M. *Inorg. Chem.* **1995**, *34*, 3358. (b) Ruminski, R. R.; Deere, P. T.; Olive, M.; Serveiss, D. *Inorg. Chim. Acta* **1998**, *281*, 1 and references therein. (c) D'Alessandro, D. M.; Kelso, L. S.; Keene, F. R. *Inorg. Chem.* **2001**, *40*, 6841.

(13) Klassen, D. M. *Inorg. Chem.* **1976**, *15*, 3166.

(14) Barigelletti, F.; Juris, A.; Balzani, V.; Belser, P.; von Zelewsky, A. *Inorg. Chem.* **1987**, *26*, 4115.

(15) (a) Rudi, A.; Kashman, Y.; Gut, D.; Lellouche, F.; Kol, M. *Chem. Commun.* **1997**, 17. (b) Gut, D.; Rudi, A.; Kopilov, J.; Goldberg, I.; Kol, M. *J. Am. Chem. Soc.* **2002**, *124*, 5449. (c) Gut, D.; Goldberg, I.; Kol, M. *Inorg. Chem.* **2003**, *42*, 3483. (d) Rudi, A.; Benayahu, I.; Goldberg, I.; Kashman, Y. *Tetrahedron Lett.* **1988**, *29*, 6655.

(99.995%) were purchased from Aldrich and used without further purification. Acetonitrile for photophysical experiments was of spectroscopic grade. All other chemicals and solvents were of reagent grade and were used without further purification, except for acetonitrile for electrochemical measurements, which was distilled over CaH_2. All reactions and electrochemical measurements were performed under an argon atmosphere.

Instrumentation. ^1H and ^{13}C NMR spectra, COSY, NOESY, and HMQC experiments were performed on a Bruker Avance 400 spectrometer using the residual protons of the solvent (CD_3CN) as an internal standard at $\delta = 1.93$ ppm. FABMS data were obtained on a VG-AutoSpec M250 mass spectrometer using a *m*-nitrobenzyl alcohol matrix. Elemental analyses were performed at the microanalytical laboratory of the Hebrew University of Jerusalem. UV/vis absorption spectra in acetonitrile were obtained on a Kontron UVIKRON 931 UV/vis spectrometer.

Cyclic and square-wave voltammetry was carried out on a μ-autolab type II potentiostat (Eco Chemie), using a platinum working electrode, a platinum auxiliary electrode, and a $Ag/AgNO_3$ (0.01 M in acetonitrile) reference electrode (Bioanalytical Systems). The measurements were carried out on the complexes dissolved in argon-purged acetonitrile containing 0.1 M tetra-*n*-butylammonium hexafluorophosphate (TBAH) as the supporting electrolyte. The typical concentration of the complexes was ca. 1.5 mM. The criteria for reversibility were the separation between the cathodic and anodic peaks (not exceeding 90 mV), the close-to-unity ratio of the intensities of the cathodic and anodic peak currents, and the constancy of the peak potential on changing scan rate. A 5 mM solution of ferrocene in acetonitrile containing 0.1 M TBAH was measured after the measurement of each complex, typically yielding a value of $E_{1/2} = 0.096$ V for Fc/Fc^+. Values were converted to the SCE scale assuming $E_{1/2} = 400$ mV for Fc/Fc^+.[18]

The luminescence spectra for ca. 2×10^{-5} M air-equilibrated acetonitrile solutions at room temperature and at 77 K were measured using an Edinburgh FLS920 spectrometer equipped with a Hamamatsu R5509-72 supercooled photomultiplier tube (193 K), a TM300 emission monochromator with an NIR grating blazed at 1000 nm, and an Edinburgh Xe900 450-W xenon arc lamp as light source. Two excitation wavelengths of 420 and 575 nm, which lead to final population of the lowest-lying emitting levels of Ru- or Os-based metal-to-ligand charge-transfer nature, were used for all complexes.[19,20] Corrected luminescence spectra in the range 700−1800 nm were obtained by using a correction curve for the phototube response provided by the manufacturer. Luminescence quantum yields (Φ) were evaluated by comparing wavelength-integrated intensities (I) with reference to $[Ru(bpy)_3]Cl_2$ ($\Phi_r = 0.028$ in air-equilibrated water)[21] or $[Os(bpy)_3](PF_6)_2$ and ($\Phi_r = 0.005$ in degassed acetonitrile)[20] as standards and by using the equation[20,22]

$$\Phi = \frac{A_r n^2 I}{n_r^2 I_r A}\Phi_r$$

where A and n are the absorbance value (<0.15) at the employed excitation wavelength and the refractive index of the solvent, respectively. Band maxima and relative luminescence intensities were obtained with uncertainties of 2 nm and 20%, respectively. The luminescence lifetimes were obtained with the same equipment operated in single-photon mode using a 407-nm laser diode excitation controlled by a Hamamatsu C4725 stabilized picosecond light pulser. Analysis of the luminescence decay profiles against time was accomplished by using software provided by the manufacturer. The lifetime values were obtained with an estimated uncertainty of 10%.

Synthesis. Isoeilatin (1). This compound was synthesized according to the published procedure.[23] Crystals suitable for X-ray analysis of the salt $[(ieil)H_2][Cl]_2$ (**1**·$[HCl]_2$) were prepared by dissolving isoeilatin (10.0 mg, 0.028 mmol) in 10 mL of CH_3OH/concentrated HCl (4:1) and allowing the solution to evaporate slowly for 2 weeks.

$[Os(bpy)_2(ieil)][PF_6]_2$ (3·$[PF_6]_2$). *rac*,*cis*-$[Os(bpy)_2Cl_2]$ (51.4 mg, 0.090 mmol) and isoeilatin (30.2 mg, 0.085 mmol) were added to 16 mL of ethylene glycol, and the mixture was heated to 100 °C for 4 h under argon atmosphere. The dark green-brown reaction mixture obtained was cooled to room temperature, and a saturated KPF_6(aq) solution was added until precipitation of a green-brown solid occurred. The solid was isolated by centrifugation and washed several times with water to remove traces of salts. The solid was dried in vacuo and was purified by chromatography on a Sephadex-CM C-25 column using a gradient of NaCl(aq)/CH_3OH (1:1) as the eluent. The mononuclear complex eluted from the column as an emerald-green band at an ionic strength of 0.1−0.15 M NaCl(aq). An additional brown band eluted at higher ionic strength [0.2−0.25 M NaCl(aq)] and was identified as the dinuclear complex $\mathbf{5}^{4+}$, yield 39% (34.1 mg as the PF_6^- salt). The appropriate fraction was precipitated by addition of a saturated KPF_6(aq) solution, filtered, and dried in vacuo. **3**·$[PF_6]_2$ was obtained as a green solid, in a yield of 28% (27.5 mg). Anal. Calcd (found) for $C_{44}H_{28}F_{12}N_8OsP_2$·$4H_2O$: C, 43.28 (43.13); H, 2.97 (2.68); N, 9.17 (9.19). ^1H NMR (CD_3CN, 323 K): δ 8.939 (d, $J = 5.0$ Hz, 1H, $H^{a'}$), 8.68 (m, 3H, $H^{c'}$, H^3, H^c), 8.586 (d, $J = 8.2$ Hz, 1H, $H^{3'}$), 8.51 (m, 2H, $H^{b'}$, $H^{3''}$), 8.320 (d, $J = 8.2$ Hz, 1H, $H^{3'''}$), 8.195 (d, $J = 6.6$ Hz, 1H, H^b), 8.126 (d, $J = 6.6$ Hz, 1H, H^a), 7.99 (m, 5H, H^4, $H^{6'}$, $H^{4''}$, H^f, $H^{4'}$), 7.85 (m, 3H, H^d, $H^{6''}$, H^e), 7.73 (m, 3H, $H^{d'}$, $H^{4'''}$, $H^{f'}$), 7.60 (m, 2H, $H^{5''}$, H^6), 7.508 (t, $J = 6.7$ Hz, 1H, H^5), 7.458 (t, $J = 7.9$ Hz, 1H, $H^{e'}$), 7.19 (m, 2H, $H^{5'}$, $H^{6'''}$), 7.065 (t, $J = 6.7$ Hz, 1H, $H^{5'''}$). ^{13}C NMR (CD_3CN, 323 K): δ 156.5 ($C-H^{6'}$), 152.9 ($C-H^{a'}$), 152.8 ($C-H^{6'''}$), 151.7 ($C-H^6$), 150.6 ($C-H^{6''}$), 149.4 ($C-H^a$), 140.2 ($C-H^4$), 139.8 ($C-H^{4''}$), 139.4 ($C-H^{4'}$), 138.9 ($C-H^{4'''}$), 133.4 ($C-H^e$), 133.1 ($C-H^{e'}$), 132.9 ($C-H^f$), 132.6 ($C-H^{d'}$), 131.5 ($C-H^d$), 129.8 ($C-H^5$), 129.7 ($C-H^{5''}$), 129.4 ($C-H^{5'}$), 129.1 ($C-H^{5'''}$), 127.4 ($C-H^{f'}$), 126.0 ($C-H^{3'}$), 125.8 ($C-H^3$), 125.7 ($C-H^{c'}$), 125.4 ($C-H^{3''}$), 125.2 ($C-H^{3'''}$), 124.9 ($C-H^c$), 123.5 ($C-H^b$), 117.7 ($C-H^{b'}$). FABMS: 860.0 $[M - 2PF_6 + H]^+$, 1002.9 $[M - PF_6]^+$.

$[\{Ru(bpy)_2\}_2\{\mu\text{-ieil}\}][PF_6]_4$ (4·$[PF_6]_4$). *rac*,*cis*-$[Ru(bpy)_2Cl_2]$·$2H_2O$ (121.5 mg, 0.233 mmol) and isoeilatin (38.5 mg, 0.108 mmol) were added to 16 mL of ethylene glycol, and the mixture was heated to 110 °C for 24 h under argon atmosphere. The green reaction mixture obtained was cooled to room temperature, and saturated KPF_6(aq) solution was added until precipitation of a green solid occurred. The solid was isolated by centrifugation and washed several times with water to remove traces of salts. The solid was dried in vacuo and was purified by recrystallization from CH_3CN/ether. The desired complex was obtained as a green solid in a yield of 93% (177.0 mg). Anal. Calcd (found) for $C_{64}H_{44}F_{24}N_{12}P_4Ru_2$·

(16) Bergman, S. D.; Reshef, D.; Frish, L.; Cohen, Y.; Goldberg, I.; Kol, M. *Inorg. Chem.* **2004**, *43*, 3792.
(17) Kober, E. M.; Caspar, J. V.; Sullivan, B. P.; Meyer, T. J. *Inorg. Chem.* **1988**, *27*, 4587.
(18) Connelly, N. G.; Geiger, W. E. *Chem. Rev.* **1996**, *96*, 877.
(19) (a) Yeh, A. T.; Shank, C. V.; McCusker, J. K. *Science* **2000**, *298*, 935. (b) Darmrauer, N. H.; Cerullo, G.; Yeh, A.; Boussie, T. R.; Shank, C. V.; McCusker, J. K. *Science* **1997**, *275*, 54.
(20) Kober, E. M.; Caspar, J. V.; Lumpkin, R. S.; Meyer, T. J. *J. Phys. Chem.* **1986**, *90*, 3722.
(21) Nakamaru, K. *Bull. Chem. Soc. Jpn.* **1982**, *55*, 2967.
(22) Demas, J. N.; Crosby, G. A. *J. Phys. Chem.* **1971**, *75*, 991.
(23) Gellerman, G.; Rudi, A.; Kashman, Y. *Tetrahedron* **1994**, *50*, 12959.

H_2O: C, 43.16 (43.14); H, 2.60 (2.63); N, 9.44 (9.33). ^{1}H NMR (CD_3CN, 298 K): δ 8.912 (d, J = 8.0 Hz, 4H, H^c_{meso}, H^c_{rac}), 8.752 (d, J = 6.5 Hz, 4H, H^b_{meso}, H^b_{rac}), 8.662 (d, J = 8.1 Hz, 2H, H^3_{rac}), 8.646 (d, J = 8.1 Hz, 2H, H^3_{meso}), 8.613 (d, J = 8.1 Hz, 4H, $H^{3'}_{meso}$, $H^{3'}_{rac}$), 8.529 (d, J = 8.0 Hz, 2H, $H^{3''}_{rac}$), 8.512 (d, J = 8.0 Hz, 2H, $H^{3''}_{meso}$), 8.397 (d, J = 8.1 Hz, 2H, $H^{3'''}_{rac}$), 8.365 (d, J = 8.4 Hz, 2H, $H^{3'''}_{meso}$), 8.313 (d, J = 6.4 Hz, 4H, H^a_{meso}, H^a_{rac}), 8.21 (m, 8H, H^4_{meso}, H^4_{rac}, $H^{4''}_{meso}$, $H^{4''}_{rac}$), 8.08 (m, 4H, $H^{4'}_{meso}$, $H^{4'}_{rac}$), 8.021 (d, J = 5.4 Hz, 2H, $H^{6''}_{rac}$), 8.00 (m, 4H, $H^{6''}_{meso}$, $H^{6'}_{meso}$), 7.97 (m, 6H, $H^{4'''}_{rac}$, H^d_{meso}, H^d_{rac}), 7.920 (d, J = 5.6 Hz, 2H, $H^{6'}_{rac}$), 7.891 (t, J = 7.8 Hz, 2H, $H^{4'''}_{meso}$), 7.838 (d, J = 8.6 Hz, 4H, H^f_{meso}, H^f_{rac}), 7.71 (m, 4H, H^6_{meso}, H^6_{rac}), 7.60 (m, 8H, $H^{5''}_{meso}$, $H^{5''}_{rac}$, H^e_{meso}, H^e_{rac}), 7.518 (t, J = 6.5 Hz, 4H, H^5_{meso}, H^5_{rac}), 7.312 (t, J = 6.8 Hz, 2H, $H^{5'}_{meso}$), 7.21 (m, 6H, $H^{6'''}_{meso}$, $H^{5'}_{rac}$, $H^{6'''}_{rac}$), 7.12 (m, 4H, $H^{5'''}_{rac}$, $H^{5'''}_{meso}$). ^{13}C NMR (CD_3CN, 298 K): δ 154.4 ($C-H^{6'}_{rac}$), 151.9 ($C-H^{6'''}_{meso}$, $C-H^{6'''}_{rac}$), 151.8 ($C-H^6_{meso}$, $C-H^6_{rac}$), 151.5 ($C-H^a_{meso}$, $C-H^a_{rac}$), 151.1 ($C-H^{6'}_{meso}$), 151.0 ($C-H^{6''}_{meso}$, $C-H^{6''}_{rac}$), 139.2 ($C-H^4_{meso}$, $C-H^4_{rac}$, $C-H^{4''}_{meso}$, $C-H^{4''}_{rac}$), 138.6 ($C-H^{4'}_{meso}$, $C-H^{4'}_{rac}$), 138.4 ($C-H^{4'''}_{meso}$, $C-H^{4'''}_{rac}$, $C-H^d_{meso}$, $C-H^d_{rac}$), 133.4 ($C-H^e_{meso}$, $C-H^e_{rac}$), 132.0 ($C-H^d_{meso}$, $C-H^d_{rac}$), 128.5 ($C-H^5_{meso}$, $C-H^5_{rac}$), 128.5 ($C-H^{5''}_{meso}$, $C-H^{5''}_{rac}$), 128.0 ($C-H^{5'''}_{meso}$, $C-H^{5'''}_{rac}$), 127.9 ($C-H^{5'}_{meso}$), 127.8 ($C-H^{5'}_{rac}$), 126.8 ($C-H^f_{meso}$, $C-H^f_{rac}$), 125.8 ($C-H^c_{meso}$, $C-H^c_{rac}$), 125.2 ($C-H^3_{meso}$, $C-H^3_{rac}$), 124.9 ($C-H^{3'}_{meso}$, $C-H^{3'}_{rac}$), 124.9 ($C-H^{3''}_{meso}$, $C-H^{3''}_{rac}$), 124.4 ($C-H^{3'''}_{meso}$, $C-H^{3'''}_{rac}$), 120.8 ($C-H^b_{meso}$, $C-H^b_{rac}$). FABMS: 1329.0 $[M - 3PF_6 + 2H]^+$, 1473.0 $[M - 2PF_6 + H]^+$, 1619.0 $[M - PF_6 + 2H]^+$.

[{Os(bpy)$_2$}$_2${μ-ieil}][PF$_6$]$_4$ (5·[PF$_6$]$_4$). This complex was prepared by the same method as described for **4**·$[PF_6]_4$, using *rac,cis*-$[Os(bpy)_2Cl_2]$ (38.5 mg, 0.067 mmol), isoeilatin (10.8 mg, 0.030 mmol), and 8 mL of ethylene glycol, and was purified by chromatography on Sephadex LH-20 using CH_3CN/CH_3OH (1:1) as the eluent. The desired complex was obtained as a brown solid, in a yield of 39% (22.9 mg). Anal. Calcd (found) for $C_{64}H_{44}F_{24}N_{12}Os_2P_4 \cdot 4H_2O$: C, 38.18 (38.26); H, 2.60 (2.47); N, 8.35 (8.24). ^{1}H NMR (CD_3CN, 298 K): δ 8.885 (d, J = 7.3 Hz, 2H, H^c_{rac}), 8.869 (d, J = 7.3 Hz, 2H, H^c_{meso}), 8.729 (d, J = 9.5 Hz, 2H, H^3_{rac}), 8.706 (d, J = 8.8 Hz, 2H, H^3_{meso}), 8.55 (m, 8H, $H^{3'}_{rac}$, $H^{3'}_{meso}$, $H^{3''}_{rac}$, $H^{3''}_{meso}$), 8.332 (d, J = 8.6 Hz, 2H, $H^{3'''}_{rac}$), 8.310 (d, J = 8.4 Hz, 2H, $H^{3'''}_{meso}$), 8.262 (d, J = 6.7 Hz, 4H, H^b_{rac}, H^b_{meso}), 8.193 (d, J = 6.6 Hz, 2H, H^a_{meso}), 8.186 (d, J = 6.6 Hz, 2H, H^a_{rac}), 8.08 (m, 4H, H^4_{rac}, H^4_{meso}), 8.022 (t, J = 7.9 Hz, 4H, $H^{4''}_{rac}$, $H^{4''}_{meso}$), 7.843 (d, J = 5.5 Hz, 2H, $H^{6''}_{meso}$), 7.829 (d, J = 5.8 Hz, 2H, $H^{6''}_{rac}$), 7.74 (m, 14H, $H^{6'}_{meso}$, $H^{4'''}_{rac}$, H^d_{rac}, H^e_{rac}, H^d_{meso}, $H^{4'''}_{meso}$, $H^{6'}_{rac}$), 7.60 (m, 18H, H^f_{rac}, H^f_{meso}, $H^{5''}_{meso}$, H^6_{meso}, H^6_{rac}, H^5_{rac}, $H^{5''}_{rac}$, H^5_{meso}, H^e_{meso}), 7.175 (t, J = 6.4 Hz, 2H, $H^{5'}_{meso}$), 7.085 (t, J = 6.3 Hz, 2H, $H^{5'}_{rac}$), 6.990 (t, J = 6.4 Hz, 4H, $H^{5'''}_{meso}$, $H^{5'''}_{rac}$), 6.936 (d, J = 5.3 Hz, 2H, $H^{6'''}_{meso}$), 6.841 (d, J = 5.6 Hz, 2H, $H^{6'''}_{rac}$). ^{13}C NMR (CD_3CN, 298 K): δ 156.1 ($C-H^{6'}_{meso}$), 156.1 ($C-H^{6'}_{rac}$), 152.8 ($C-H^{6'''}_{rac}$), 152.7 ($C-H^{6'''}_{meso}$), 152.2 ($C-H^6_{meso}$, $C-H^6_{rac}$), 151.6 ($C-H^a_{meso}$, $C-H^a_{rac}$), 150.9 ($C-H^{6''}_{meso}$, $C-H^{6''}_{rac}$), 140.8 ($C-H^{4''}_{meso}$, $C-H^{4''}_{rac}$), 140.7 ($C-H^4_{rac}$, $C-H^4_{meso}$), 139.9 ($C-H^{4'}_{rac}$, $C-H^{4'}_{meso}$), 139.7 ($C-H^{4'''}_{rac}$), 139.4 ($C-H^{4'''}_{meso}$), 133.6 ($C-H^e_{meso}$), 133.5 ($C-H^e_{rac}$), 129.9 ($C-H^{5''}_{meso}$, $C-H^5_{rac}$, $C-H^{5''}_{rac}$, $C-H^5_{meso}$), 129.8 ($C-H^f_{rac}$, $C-H^f_{meso}$), 129.5 ($C-H^{5'}_{meso}$), 129.4 ($C-H^{5'}_{rac}$), 129.2 ($C-H^{5'''}_{meso}$, $C-H^{5'''}_{rac}$), 128.1 ($C-H^d_{rac}$, $C-H^d_{meso}$), 126.2 ($C-H^3_{rac}$, $C-H^3_{meso}$), 126.1 ($C-H^c_{rac}$, $C-H^c_{meso}$), 126.1 ($C-H^{3'}_{rac}$, $C-H^{3'}_{meso}$), 125.7 ($C-H^{3''}_{rac}$, $C-H^{3''}_{meso}$), 125.3 ($C-H^{3'''}_{rac}$, $C-H^{3'''}_{meso}$), 122.7 ($C-H^b_{rac}$, $C-H^b_{meso}$). FABMS, 1507.1 $[M - 3PF_6 + 2H]^+$, 1652.0 $[M - 2PF_6 + 2H]^+$, 1796.8 $[M - PF_6 + H]^+$.

[{(bpy)$_2$Ru}{μ-ieil}{Os(bpy)$_2$}][PF$_6$]$_4$ (6·[PF$_6$]$_4$). *rac,cis*-$[Os(bpy)_2Cl_2]$ (27.0 mg, 0.047 mmol) and **2**·$[Cl]_2$ (29.4 mg, 0.035 mmol) were added to 18 mL of ethylene glycol, and the mixture was heated to 130 °C for 5 days under argon atmosphere. The red-brown reaction mixture obtained was cooled to room temperature, and saturated KPF_6(aq) solution was added until precipitation of a dark solid occurred. The solid was isolated by centrifugation and washed several times with water to remove traces of salts. The solid was dried in vacuo and then purified by chromatography on a Sephadex LH-20 column using CH_3CN/CH_3OH (1:1) as the eluent. The appropriate dark olive-green fraction was collected, and the solvent was removed in vacuo. The desired complex was obtained as a dark olive-green solid, yield 39% (25.4 mg). Anal. Calcd (found) for $C_{64}H_{44}F_{24}N_{12}OsP_4Ru \cdot 2H_2O$: C, 40.71 (40.88); H, 2.56 (2.84); N, 8.90 (8.67). FABMS: 1415.8 $[M - 3PF_6]^+$, 1563.7 $[M - 2PF_6 + 2H]^+$, 1707.7 $[M - PF_6 + H]^+$.

X-ray Structure Determinations. X-ray diffraction measurements were carried out at ca. 110 K on a Nonius Kappa CCD diffractometer using Mo Kα (λ = 0.7101 Å) radiation. To minimize thermal motion effects, solvent disorder, and deterioration, the analyzed crystals were embedded within a drop of amorphous viscous oil and freeze-cooled to 110 K. Intensity data were corrected for absorption. The crystal structures were solved by Patterson and Fourier techniques (DIRDIF-96)[24] and direct methods (SIR-97)[25] and refined by full-matrix least-squares (SHELXL-97).[26]

Crystal Data for 1·[HCl]$_2$: $C_{24}H_{12}N_4 \cdot 2HCl \cdot 2H_2O$, formula weight 465.32, triclinic, space group $P\bar{1}$, a = 7.5880(3) Å, b = 8.0250(3) Å, c = 8.9980(4) Å, α = 81.321(3)°, β = 78.132(2)°, γ = 73.8420(18)°, V = 512.46(4) Å^3, Z = 1, D_{calc} = 1.508 g·cm^{-3}, $F(000)$ = 240, μ(Mo Kα) = 3.49 cm^{-1}, crystal size 0.30 × 0.15 × 0.10 mm, θ_{max} = 25.68°, 1901 unique reflections. R1 = 0.0439 and wR2 = 0.1100 for 1614 reflections with $I > 2\sigma(I)$, and R1 = 0.0544 and wR2 = 0.1175 for all data. The N-bonded protons were located from diffraction data on difference Fourier maps. The asymmetric unit of this structure consists of one unit of the biprotonated isoeilatin ligand located on an inversion center, two Cl^- counterions (one of them partly disordered), and two molecules of water.

Crystal Data for *meso*-4·[PF$_6$]$_4$: $C_{64}H_{44}F_{24}N_{12}P_4Ru_2 \cdot 2H_2O \cdot 2CH_3CN$, formula weight 1881.27, triclinic, space group $P\bar{1}$, a = 11.1200(3) Å, b = 12.6530(3) Å, c = 13.9580(5) Å, α = 94.2320(10)°, β = 97.7970(10)°, γ = 110.9131(11)°, V = 1801.65(9) Å^3, Z = 1, D_{calc} = 1.734 g·cm^{-3}, $F(000)$ = 940, μ(Mo Kα) = 6.28 cm^{-1}, crystal size 0.33 × 0.15 × 0.15 mm, θ_{max} = 27.86°, 7618 unique reflections. R1 = 0.0703 and wR2 = 0.1793 for 5942 reflections with $I > 2\sigma(I)$, and R1 = 0.0923 and wR2 = 0.1976 for all data. The asymmetric unit of this structure consists of one unit of the complex located on a center of inversion, four PF_6^- counterions (one of them partly disordered), one molecule of water solvent, and one positionally and orientationally disordered acetonitrile solvent molecule.

Crystal Data for *meso*-4·[Cl]$_4$: $C_{64}H_{44}Cl_4N_{12}Ru_2 \cdot 2H_2O \cdot 6CH_3CN$, formula weight 1607.41, monoclinic, space group $P2_1/c$, a = 9.1930(3) Å, b = 26.2950(6) Å, c = 15.3130(6) Å, β = 97.9360(12)°, V = 3666.2(2) Å^3, Z = 2, D_{calc} = 1.456 g·cm^{-3}, $F(000)$ = 1640, μ(Mo Kα) = 6.18 cm^{-1}, crystal size 0.20 × 0.20 × 0.10

(24) Beurskens, P. T.; Beurskens, G.; Bosman, W. P.; de Gelder, R.; Garcia-Granda, S.; Gould, R. O.; Israel, R.; Smits, J. M. M. *DIRDIF-96*; Crystallography Laboratory, University of Nijmegen: Nijmegen, The Netherlands, 1996.

(25) Altomare, A.; Burla, M. C.; Camalli, M.; Cascarano, M.; Giacovazzo, C.; Guagliardi, A.; Polidori, G. SIR-97. *J. Appl. Crystallogr.* **1994**, *27*, 435.

(26) Sheldrick, G. M. *SHELXL-97. Program for the Refinement of Crystal Structures from Diffraction Data*; University of Göttingen: Göttingen, Germany, 1997.

Scheme 1. Synthesis of the Mononuclear and Dinuclear Complexes of Isoeilatin **2**−**6**

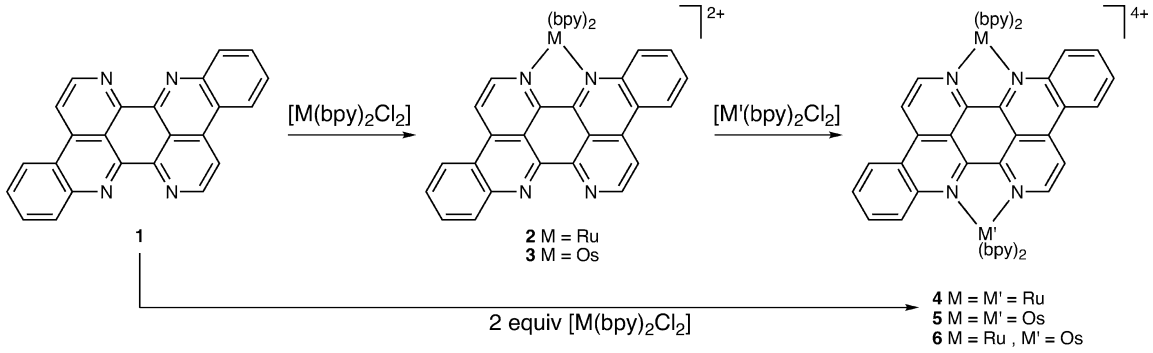

mm, $\theta_{max} = 28.13°$, 8745 unique reflections. R1 = 0.0645 and wR2 = 0.1603 for 5899 reflections with $I > 2\sigma(I)$, and R1 = 0.1073 and wR2 = 0.1854 for all data. The structure contains four molecules of partly disordered water and an unknown number (estimated to be 12) of severely disordered acetonitrile molecules as the crystallization solvent. All of the molecules of the complex are located on centers of inversion.

Crystal Data for *meso*-5·[PF$_6$]$_4$: $C_{32}H_{22}F_{12}N_6OsP_2 \cdot H_2O \cdot CH_3CN$, formula weight 1029.77, triclinic, space group $P\bar{1}$, a = 11.1590(5) Å, b = 12.6670(5) Å, c = 13.9510(6) Å, α = 94.184(3)°, β = 97.4710(19)°, γ = 111.128(3)°, V = 1808.44(13) Å^3, Z = 2, D_{calc} = 1.891 g·cm^{-3}, $F(000)$ = 1004, μ(Mo Kα) = 37.18 cm^{-1}, crystal size 0.20 × 0.15 × 0.15 mm, θ_{max} = 27.00°, 7330 unique reflections. R1 = 0.0388 and wR2 = 0.0932 for 6311 reflections with $I > 2\sigma(I)$, and R1 = 0.0496 and wR2 = 0.0987 for all data. The asymmetric unit of this structure consists of the osmium salt, one molecule of water solvent molecule whose protons could not be located, and one disordered acetonitrile solvent molecule.

The apparent solvent/anion disorder in *meso*-**4**·[PF$_6$]$_4$, *meso*-**4**·[Cl]$_4$, and *meso*-**5**·[PF$_6$]$_4$ has little effect on the molecular structures of the corresponding isoeilatin complexes.

NMR Dimerization Experiments. Typically, a concentrated stock solution (ca. 10 mM) of a complex was prepared by accurately weighing the dried compound and dissolving it in an accurately measured volume of CD_3CN (1.00−2.00 mL). The concentration dependence of the chemical shifts was studied at constant temperature, measured by the chemical shift of MeOH. Fifty-microliter aliquots of the stock solution were added to an NMR tube initially containing 0.40 mL of CD_3CN, and 50-μL aliquots of CD_3CN were added to an NMR tube initially containing 0.40 mL of the stock solution to obtain a broad concentration range. The NMR spectra were recorded after several minutes of thermal equilibration time following each addition. The dimerization constants were calculated, based on the chemical shifts of protons H^b, H$^{b'}$, H^c, and H$^{c'}$, by the method of Horman and Dreux.[27]

Results and Discussion

Syntheses. The mononuclear complexes **2**$^{2+}$ and **3**$^{2+}$ were prepared by reacting **1** with 1.0−1.1 equiv of the appropriate metal precursor *rac*,*cis*-[M(bpy)$_2$Cl$_2$] (M = Ru, Os) in ethylene glycol at 100 °C, as shown in Scheme 1. The complexes were purified by column chromatography on Sephadex-CM C-25 and isolated as the PF_6^- salts. The homodinuclear complexes were obtained as byproducts in the preparation of the mononuclear counterparts and were also prepared independently.

The direct synthesis of the homodinuclear complexes **4**$^{4+}$ and **5**$^{4+}$ involved reacting **1** with ca. 2.5 equiv of *rac*,*cis*-[M(bpy)$_2$Cl$_2$] (M = Ru, Os) in ethylene glycol at 110 °C (Scheme 1). The complexes were isolated as the PF_6^- salts and purified either by recrystallization from CH_3CN/ether or by chromatography on Sephadex LH-20. The heterodinuclear complex **6**$^{4+}$ was prepared by reacting **2**·[Cl]$_2$ with 1.5 equiv of *rac*,*cis*-[Os(bpy)$_2$Cl$_2$] in ethylene glycol at 130 °C; **6**$^{4+}$ was isolated as the PF_6^- salt and purified by column chromatography on Sephadex LH-20. All complexes were characterized by 1D and 2D NMR techniques, by MS, and by elemental analysis.

NMR Spectroscopy. The NMR characterization of all of the complexes as the PF_6^- salts in CD_3CN was achieved by utilization of COSY, NOESY, and HMQC two-dimensional NMR techniques. The ^{1}H NMR spectra of all of the mononuclear complexes exhibit 12 signals corresponding to the isoeilatin ligand, bound at only one of its two available coordination sites. The spectra are characterized by a well-separated low field doublet, appearing at 8.9−9.5 ppm, corresponding to the isoeilatin H$^{a'}$ proton. The identification of the bound side of the ligand was accomplished by NOESY spectra, which exhibited NOE correlations between the bpy H^6 protons and the isoeilatin H^a and H$^{f'}$ protons. Additional support for this assignment was obtained from the concentration-dependence behavior of the various peaks (vide infra), as the isoeilatin protons from the bound side of the ligand, i.e., H^a and H$^{f'}$, exhibited negligible shifts as a function of concentration, given that they are outside the effective π-stacking area. The connectivity between adjacent pyrido and benzo rings in the isoeilatin ligand could be established similarly from the NOE correlation between the appropriate H^b and H^c protons. Because of the C_1 symmetry of the complexes, the four pyridyl rings of the bpy ligands are nonequivalent. In both cases, the H^3 to H^6 protons of each pyridyl ring show the normal coupling patterns, and the connectivity between them was established by NOESY spectra, which showed clear NOE correlations between the appropriate H^3 protons.

As previously reported for **2**$^{2+}$,[16] complex **3**$^{2+}$ exhibits concentration- and temperature-dependent ^{1}H NMR spectra, as illustrated in Figure 2. This dependence results from the formation of discrete dimers in solution held together by

(27) Horman, I.; Dreux, B. *Helv. Chim. Acta* **1984**, *67*, 754.

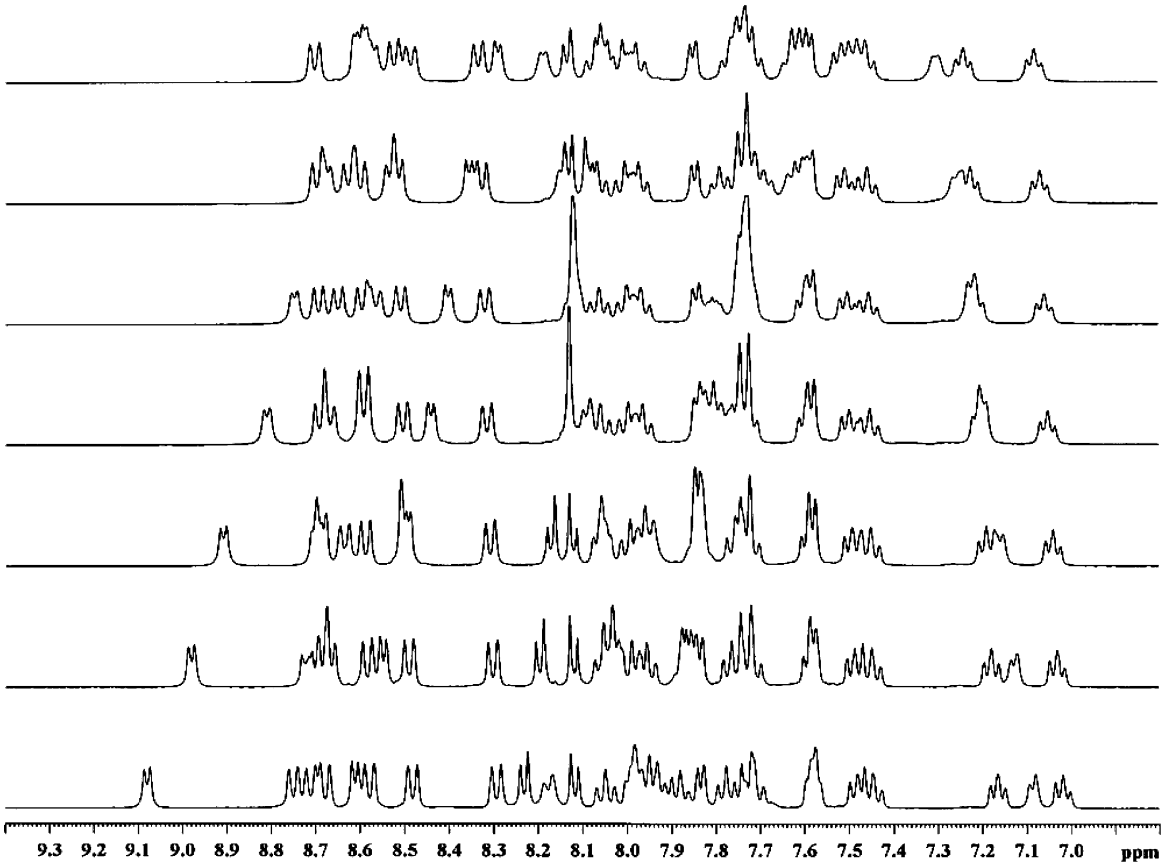

Figure 2. ^{1}H NMR spectra of **3**·$[PF_6]_2$ in CD_3CN at various concentrations, from top to bottom: 7.94, 6.11, 4.96, 4.25, 3.31, 2.71, and 1.98 mM.

π-stacking interactions via the isoeilatin ligand. Only one of the four bpy H^6 protons exhibits marked shifts, indicating the same face selectivity as observed for $\mathbf{2}^{2+}$, namely, that only one of the faces of the isoeilatin complex is "sticky". Assuming that the π-stacking interaction occurs over the maximal overlap area, it follows that heterochiral dimer formation is preferred over homochiral dimer formation. The strength of the π-stacking can be quantified in terms of the dimerization constant, which was calculated from the NMR data to be $K_d = 72 \pm 5\ M^{-1}$. This value is slightly higher than that reported for $\mathbf{2}^{2+}$ but is still significantly lower than that observed for the corresponding eilatin complex ($K_d = 310\ M^{-1}$),[15b] emphasizing that the different skeletal arrangement of the rings exerts a profound effect on the π-stacking of the ligand.

The ^{1}H NMR spectra of the homodinuclear complexes $\mathbf{4}^{4+}$ and $\mathbf{5}^{4+}$ are highly complicated because of the presence of two diastereoisomeric forms: meso ($\Delta\Lambda$) and rac ($\Delta\Delta/\Lambda\Lambda$). The meso and rac forms are of C_i and C_2 symmetry, respectively, and therefore give rise to a total of 44 signals. In contrast to the analogous dibenzoeilatin complexes, whose diastereoisomers exhibited only small differences in the NMR spectra,[11b,28] the meso and rac forms of the isoeilatin complexes exhibit noticeable differences, most conveniently observed for the protons of the peripheral bpy ligands. According to ^{1}H NMR integral ratios, the homodinuclear complexes $\mathbf{4}^{4+}$ and $\mathbf{5}^{4+}$ were obtained in meso/rac compositions of 3/1 and 3/2, respectively. The heterodinuclear complex $\mathbf{6}^{4+}$, formed as a mixture of heterochiral ($\Delta\Lambda/\Lambda\Delta$) and homochiral ($\Delta\Delta/\Lambda\Lambda$) diastereoisomers, both of which are of C_1 symmetry, gives rise to a total of 88 signals. The ^{1}H NMR spectrum of $\mathbf{6}^{4+}$ is too complex to be solved completely; however, from the integral ratios of several high-field signals, which are identified as bpy $H^{6'''}$ protons, it was possible to determine that the heterochiral/homochiral composition is 3/2.

The ^{1}H NMR spectra of the dinuclear complexes show a slight concentration dependence, being most noticeable for protons H^d and H^e. Because these complexes are stoppered by two bulky $Ru(bpy)_2$ termini that prevent face-to-face approach of the isoeilatin moieties, the only viable pathway for π-stacking is by "side approach", where the benzo rings of the isoeilatin ligand stick out from the shielded area. This is consistent with the NMR data and is supported by the crystal structure (vide infra).

Structure. Several unsuccessful attempts to crystallize **1** prompted us to try a different approach, i.e., crystallization of its salt. Isoeilatin in its protonated form is much more soluble in common organic solvents, and its structure would be indicative of the structure of the unprotonated form. We were able to obtain X-ray-quality crystals of the salt **1**·$[HCl]_2$ by recrystallizaing **1** from a mixture of methanol and concentrated hydrochloric acid (see Experimental Section). A perspective view (ORTEP) of the cation $\mathbf{1}\cdot 2H^+$ with partial

(28) D'Alessandro, D. M.; Keene, F. R.; Bergman, S. D.; Kol, M. *Dalton Trans.* **2005**, 332.

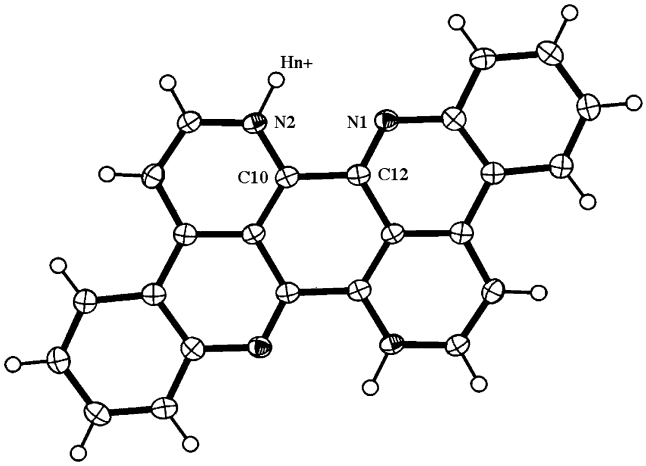

Figure 3. ORTEP view of **1**·$[HCl]_2$ with partial atom labeling. Counteranions and solvent molecules are omitted for clarity.

atom numbering is shown in Figure 3. **1**·$[HCl]_2$ crystallized in a triclinic unit cell of the space group $P\bar{1}$, the asymmetric unit containing one molecule of isoeilatin that is protonated on two of its nitrogen atoms and is located on an inversion center, two chloride counterions, and two molecules of water. The protonation of the nitrogen atoms on the less substituted ring can be correlated with the higher basicity of pyridine relative to quinoline. Despite the double protonation, the isoeilatin moiety preserves its planarity, thus structurally resembling the unprotonated **1**. The crystal structure of **1**·$[HCl]_2$ consists of layers of tightly stacked molecules of the biprotonated isoeilatin. These layers extend throughout the crystal parallel to the *ab* plane and center at $z = 0$ (Figure S1, see Supporting Information). Neighboring layers are related by crystallographic translation along the *c* axis, entrapping the chloride anions and water molecules in the intermediate zones. The latter bridge by hydrogen bonding between the protonated *N* sites and chloride anions. The nearly perfectly planar aromatic moieties stack in an offset manner in order to optimize $\pi-\pi$ attraction and avoid electrostatic repulsion between the central protonated fragments, the intralayer organization resembling a perfect brick wall. Every molecule is thus in close contact with four neighboring species from above and below that are related to it by crystallographic translation of $\pm b$ and $\pm(a - b)$. The relatively short interplanar distances between the overlapping fragments (3.35 and 3.31 Å) are indicative of a rather strong stacking interaction.

Semiempirical MO calculations have shown that protonation of the structurally related eilatin ligand would proceed spontaneously up to the doubly protonated form; further protonation is energetically disfavored because of the inevitable distortion of the ligand.[29] In addition, of the four possible biprotonated isomers that can form, the most stable is the one where the eilatin is protonated on one bpy-head nitrogen and on one biq-tail nitrogen on opposite sides of the ligand ("trans" to each other). This is consistent with our results concerning the isoeilatin ligand, which is also obtained in the biprotonated form as the trans isomer, as confirmed by precise X-ray diffraction analysis.

(29) Sato, T.; Kataoka, M. *J. Chem. Res. (S)* **1998**, 542.

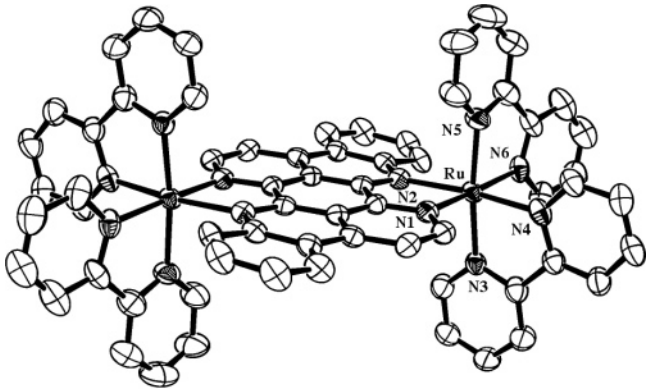

Figure 4. ORTEP view of *meso*-**4**·$[PF_6]_4$ with partial atom labeling. Counterions and solvent molecules are omitted for clarity.

Table 1. Metal-to-Metal Distances and Selected Bond Lengths (Å) and Angles (deg) for *meso*-**4**·$[Cl]_4$, *meso*-**4**·$[PF_6]_4$, and *meso*-**5**·$[PF_6]_4$

	meso-**4**·$[Cl]_4$	*meso*-**4**·$[PF_6]_4$	*meso*-**5**·$[PF_6]_4$
M···M	8.05	8.08	8.08
M−N(1)	2.029	2.045	2.038
M−N(2)	2.122	2.126	2.104
M−N(3)	2.053	2.062	2.060
M−N(4)	2.064	2.052	2.057
M−N(5)	2.058	2.061	2.065
M−N(6)	2.066	2.094	2.113
N(1)−M−N(2)	79.13	78.46	78.54
N(3)−M−N(4)	79.17	79.81	78.69
N(5)−M−N(6)	78.54	79.30	78.56

We have published in a preliminary report the crystal structure of $\mathbf{2}^{2+}$, as both the PF_6^- and Cl^- salts.[16] The two structures exhibited the same features: discrete heterochiral dimers held together by π-stacking interactions via the isoeilatin moiety, where the isoeilatin ligands are oriented long axis to long axis, and dimerization occurs through only one particular isoeilatin face. To date, we have not been able to obtain crystals of $\mathbf{3}^{2+}$ suitable for X-ray analysis; we assume that the structural features of this ion are similar to those observed for $\mathbf{2}^{2+}$.

The complex *meso*-**4**·$[Cl]_4$ was crystallized in a monoclinic $P2_1/c$ unit cell by slow evaporation of a concentrated acetonitrile solution, whereas both *meso*-**4**·$[PF_6]_4$ and *meso*-**5**·$[PF_6]_4$ were crystallized in triclinic $P\bar{1}$ unit cells from CH_3CN/CH_3OH. The representative perspective views (ORTEP) of the dinuclear complexes *meso*-**4**·$[PF_6]_4$ and *meso*-**5**·$[PF_6]_4$ with partial atom numbering are shown in Figures 4 and S2 (Supporting Information), respectively; selected bond distances and angles are given in Table 1. For all three structures, the asymmetric unit contains one-half of a complex molecule located on a center of inversion, two counteranions (chloride or hexafluorophosphate), and the appropriate molecules of the crystallization solvent (water and/or acetonitrile). All three structures exhibit similar features, regarding the metal-to-metal distance (ca. 8.1 Å) and the slight asymmetry in the M−N bond lengths for the pyrido N(1) and quinoline N(2) of the isoeilatin ligand (although the M−N bond distances are comparable to those reported for Ru/Os polypyridyl complexes[30,31]). The crystal

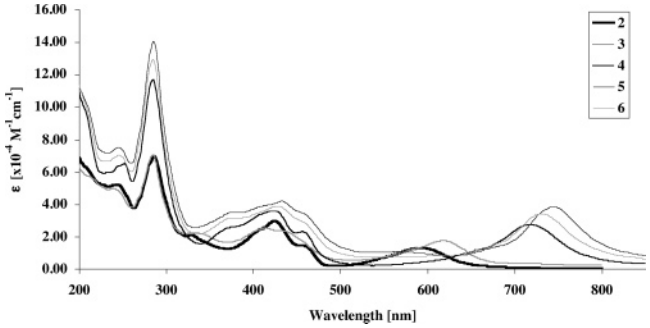

Figure 5. Absorption spectra of the mononuclear complexes $\mathbf{2}^{2+}$ (double bold black line) and $\mathbf{3}^{2+}$ (bold gray line) and of the dinuclear complexes $\mathbf{4}^{4+}$ (bold black line), $\mathbf{5}^{4+}$ (gray line), and $\mathbf{6}^{4+}$ (black line), recorded in acetonitrile.

packing of both *meso*-**4**·$[PF_6]_4$ and *meso*-**5**·$[PF_6]_4$ excludes any interaction between the complex molecules. However, the tight packing in the solid state of *meso*-**4**·$[Cl]_4$ leads to partial side stacking of the isoeilatin moieties via their benzo rings (with an interplanar distance of 3.47 Å), which are relatively unshielded by the peripheral bpy ligands and therefore stick out (Figure S3, Supporting Information). The slight concentration dependence of the NMR spectra of the dinuclear species, despite the presence of two bulky $M(bpy)_2$ termini (vide supra), indicates that some stacking occurs in solution as well. The protons that are most affected by changes in concentration, i.e., H^d and H^e, support the notion that the stacking of the dinuclear complexes in solution occurs in a side fashion similar to that observed in the solid state.

Most notable is the preservation of the planarity of the bridging isoeilatin. This stands in sharp contrast to analogous eilatin complexes, where substantial distortion from planarity occurs upon binding of the second metal fragment. The diastereoisomeric preference observed in the preparation of the dinuclear isoeilatin complexes cannot be rationalized by steric interactions between the peripheral bpy ligands, as the metal atoms are relatively remote.[32] A possible explanation relies on the asymmetry of the pq-type coordination site that induces a certain preference according to the chirality of the already-bound metal fragment.

Absorption Spectra. The UV/vis spectra of all complexes as the PF_6^- salts were recorded in acetonitrile (such measurements could not be performed for isoeilatin because of its insolubility); absorption spectra are illustrated in Figure 5, and absorption data listing energy maxima and absorption coefficients are summarized in Table 2. The assignments of the absorption bands were based on the well-documented optical transitions of $[Ru(bpy)_3]^{2+}$ and $[Os(bpy)_3]^{2+}$ [3a,5b,33] and were supported by electrochemical measurements (vide infra). For the dinuclear complexes, the results are reported for the mixture of the two diastereoisomers.

Table 2. Absorption Data[a]

complex	absorption maxima λ_{max}, nm ($\epsilon \times 10^{-4}$, $M^{-1}cm^{-1}$)
$[Ru(bpy)_3]^{2+}$ [b]	250 (2.5), 285 (8.7), 323 sh, 345 sh, 452 (1.4)
$[Os(bpy)_3]^{2+}$ [c]	290 (7.8), 436 (1.1), 478 (1.1), 579 (0.3)
$\mathbf{2}^{2+}$ [d]	243 (5.2), 285 (5.5), 328 (2.1), 410 sh, 424 (3.0), 556 sh, 593 (1.3)
$\mathbf{3}^{2+}$	240 (4.8), 285 (6.7), 331 (2.1), 414 (2.4), 442 sh, 575 sh, 620 (1.6)
$\mathbf{4}^{4+}$	258 (5.7), 289 (10.3), 380 sh, 425 (3.6), 457 (2.2), 640 sh, 718 (2.7)
$\mathbf{5}^{4+}$	245 (7.0), 286 (11.8), 378 (3.3), 410 sh, 433 (3.9), 460 sh, 564 (0.9), 685 sh, 743 (3.7)
$\mathbf{6}^{4+}$	246 (6.8), 286 (9.8), 381 sh, 427 (3.8), 462 sh, 675 sh, 731 (3.4)

[a] Recorded in acetonitrile for the complexes as PF_6^- salts. [b] From ref 3a. [c] From refs 5b and 33. [d] From ref 16.

The absorption spectra of the mononuclear complexes exhibit intense absorption bands in the UV region (200−350 nm), assigned to ligand-centered (LC) $\pi \rightarrow \pi^*$ transitions of the peripheral bpy ligands. In the visible region, the band centered around 420 nm is assigned to isoeilatin-centered $\pi \rightarrow \pi^*$ transitions, overlapping with $d_\pi(M) \rightarrow \pi^*$(bpy) metal-to-ligand charge-transfer (MLCT) transitions. In addition, the spectra exhibit broad low-lying absorption bands centered around 600 nm, assigned to $d_\pi(M) \rightarrow \pi^*$(ieil) MLCT transitions. The combination of absorptions at 600 and 420 nm renders these complexes their dark green color. A red-shifting of the $d_\pi(M) \rightarrow \pi^*$(ieil) MLCT transition is observed on going from $\mathbf{2}^{2+}$ to $\mathbf{3}^{2+}$ (593 and 620 nm, respectively), as expected for the higher-lying d_π(Os) orbitals.

Coordination of a second metal fragment brings about a pronounced red-shifting (ca. 100 nm) of the $d_\pi(M) \rightarrow \pi^*$-(ieil) MLCT transition through stabilization of the isoeilatin-centered π^* orbital. As observed for the mononuclear complexes, changing the metal center from Ru to Os causes a red-shifting of the $d_\pi(M) \rightarrow \pi^*$(ieil) MLCT band, occurring at 718 nm for $\mathbf{4}^{4+}$, 731 nm for $\mathbf{6}^{4+}$, and 743 nm for $\mathbf{5}^{4+}$. This shifting is responsible for the observed color change to yellow-green (complexes $\mathbf{4}^{4+}$ and $\mathbf{6}^{4+}$) and brown (complex $\mathbf{5}^{4+}$). All of the dinuclear complexes exhibit higher extinction coefficients than the corresponding monometallic species, as expected by the addition of a second chromophoric $M(bpy)_2^{2+}$ unit, as well as a broadened absorption around 420 nm, spanning from 350 to 500 nm. All other features of the absorption spectra of the dinuclear complexes are similar to those of their mononuclear counterparts.

Electrochemistry. The redox behavior of all of the complexes as the PF_6^- salts was studied in acetonitrile solution, employing cyclic and square-wave voltammetry techniques. $E_{1/2}$ values of successive closely spaced reduction processes were determined using the peak potential value (E_p) from the square-wave voltammograms. The results are collected in Table 3, together with the data on $[Ru(bpy)_3]^{2+}$ and $[Os(bpy)_3]^{2+}$ obtained under the same conditions;[3a,34] representative square-wave voltammograms are shown in Figure 6. For the dinuclear complexes, the results are reported for the mixture of the two diastereoisomers.

(30) (a) Shklover, V.; Zakeeruddin, S. M.; Nesper, R.; Fraser, D.; Grätzel, M. *Inorg. Chim. Acta* **1998**, *274*, 64. (b) Richter, M. M.; Scott, B.; Brewer, K. J.; Willett, R. D. *Acta Crystallogr. C* **1991**, *47*, 2443.
(31) Breu, J.; Stoll, A. *J. Acta Crystallogr. C* **1996**, *52*, 1174.
(32) It has been reported that molecular modeling of the diastereoisomers of dinuclear azobis(4-methyl-2-pyridine) complexes revealed possible interligand interactions in the rac form, which might explain the apparent preferential formation of the meso isomer. See: Kelso, L. S.; Reitsma, D. A.; Keene, F. R. *Inorg. Chem.* **1996**, *35*, 5144.
(33) Börje, A.; Köthe, O.; Juris, A. *J. Chem. Soc., Dalton Trans.* **2002**, 843.

Table 3. Half-Wave Potentials for the Oxidation and Reduction of the Complexes[a]

complex	$Ru^{II/III}$	$Os^{II/III}$	E_{red1}	E_{red2}	E_{red3}	k_{com}[g]
$[Ru(bpy)_3]^{2+}$ [b]	1.28		−1.33	−1.53	−1.78	
$[Os(bpy)_3]^{2+}$ [c]		0.81	−1.29	−1.46	−1.79	
$\mathbf{2}^{2+}$ [d]	1.42 (60)		−0.40 (110)	−0.90 (110)	−1.56[e,f]	
$\mathbf{3}^{2+}$		1.03 (60)	−0.41 (80)	−0.87 (80)	−1.52[e,f]	
$\mathbf{4}^{4+}$	1.47 (90)	1.63 (80)	−0.04 (70)		−0.51 (70)	0.5×10^3
$\mathbf{5}^{4+}$		1.03 (60)	1.29 (60)	−0.09 (60)	−0.49 (60)	2.5×10^4
$\mathbf{6}^{4+}$	1.60 (60)	1.11 (60)		−0.07 (60)	−0.50 (60)	−1.45[e,f]

[a] Potentials are given vs SCE in acetonitrile, with 0.1 M n-Bu_4NPF_6 as the supporting electrolyte, measured at room temperature with a scan rate of 0.1 V/s. ΔE_p values (mV) are given in parentheses. [b] From ref 3a. [c] From ref 34. [d] From ref 16. [e] Values determined from square-wave voltammetry. [f] Unresolved processes. [g] Calculated using $k_{com} = \exp(nF\Delta E/RT)$, where $T = 298$ K and ΔE is the separation between the two oxidation processes (see ref 4b).

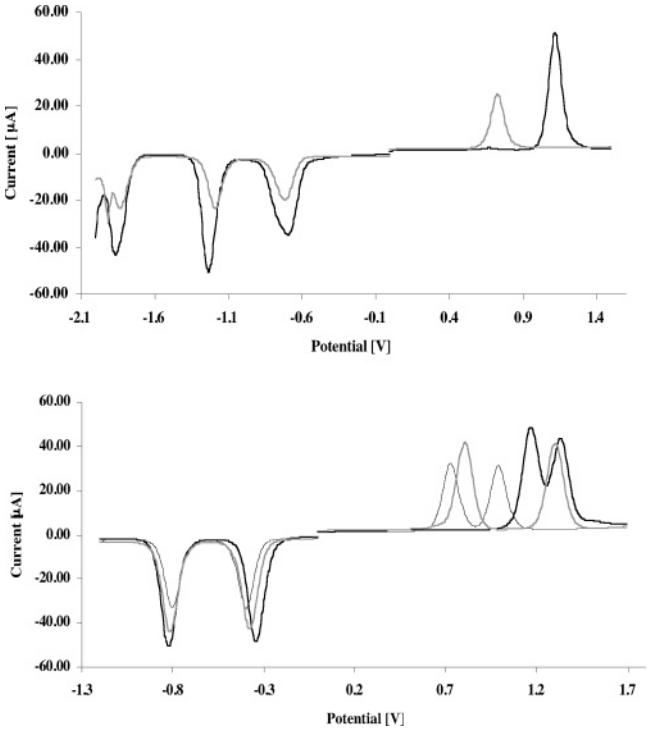

Figure 6. (Top) Square-wave voltammograms of the mononuclear complexes $\mathbf{2}^{2+}$ (black line) and $\mathbf{3}^{2+}$ (gray line), vs $Ag/AgNO_3$. (Bottom) Square-wave voltammograms of the dinuclear complexes $\mathbf{4}^{4+}$ (bold black line), $\mathbf{5}^{4+}$ (black line), and $\mathbf{6}^{4+}$ (bold gray line) vs $Ag/AgNO_3$.

The mononuclear complexes display a single reversible metal-centered oxidation ($M^{II/III}$), as well as several successive one-electron ligand-centered reductions. The oxidation potential of the metal center in $\mathbf{2}^{2+}$ is anodically shifted with respect to that of $[Ru(bpy)_3]^{2+}$ (1.42 compared to 1.28 V vs SCE, respectively). Similarly, the oxidation potential of the Os center in $\mathbf{3}^{2+}$ is anodically shifted with respect to that of $[Os(bpy)_3]^{2+}$ (1.03 compared to 0.81 V vs SCE). This is explained by the strong π-acceptor character of the isoeilatin ligand that stabilizes the $d_\pi(M)$ orbitals. Also, the more facile oxidation of $\mathbf{3}^{2+}$ compared to $\mathbf{2}^{2+}$ is consistent with the higher-lying metal-centered orbitals in Os. The first and second reversible one-electron reduction waves, appearing at around −0.4 and −0.9 V, respectively, appear at significantly anodically shifted potentials compared to those of $[Ru(bpy)_3]^{2+}$ and $[Os(bpy)_3]^{2+}$. Therefore, these two reduction processes are attributed to two consecutive reductions of the isoeilatin ligand, consistent with its low-lying π^* orbital. Additional reduction waves attributed to reduction of the peripheral bpy ligands appear at more cathodic potentials but are ill-resolved because of desorption peaks.

Comparison of the absorption and electrochemical data for eilatin-type complexes of the general formula $[M(bpy)_2(Lig)]^{2+}$ (M = Ru, Os; Lig = eilatin,[15b,15c] dibenzoeilatin,[11b] isoeilatin) reveals that all of these complexes exhibit closely related absorption maxima (the maximum difference being ca. 10 nm) and redox potentials (the maximum difference being ca. 0.1 V). It would thus appear that the electronic properties of these complexes are determined, to a large extent, by the tetraazaperylene core.[35] The addition of benzo rings, their number, relative position, and their distortion from planarity, have very little effect on the characteristics of the frontier orbitals.

As noted above for the absorption spectra, coordination of a second metal fragment further lowers the energy of the π^*(ieil) orbital, leading to a substantial anodic shift of the bridging ligand's reduction potentials. The first reversible one-electron reduction wave of isoeilatin, occurring at ca. −0.05 V vs SCE, is substantially anodically shifted (ca. 0.3 V) compared to the first reduction process of the corresponding mononuclear complex. An additional reversible one-electron reduction wave of the bridging isoeilatin occurs at ca. −0.50 V vs SCE. Subsequent reductions of the peripheral bpy ligands are unresolved because of desorption peaks.

The homodinuclear complexes exhibit two reversible, well-resolved metal-centered oxidations, despite the chemical equivalence of the metal ions. The first oxidation process occurs at potentials comparable to those of the mononuclear complexes. The second oxidation process is anodically shifted, the difference between the two oxidation processes being 0.16 V for $\mathbf{4}^{4+}$ and 0.26 V for $\mathbf{5}^{4+}$. The separation between the half-wave potentials of the two oxidation processes (ΔE) is a measure of the extent of electronic coupling between them.[36] The metal-to-metal distance in the dinuclear complexes (ca. 8.1 Å) is unlikely to permit through-space coupling. The metal−metal interaction can be explained on the basis of superexchange theory,[4] where the overlap between the metal orbitals is mediated by the orbitals of the bridging ligand. The larger ΔE observed in $\mathbf{5}^{4+}$ compared to $\mathbf{4}^{4+}$ is consistent with an electron-transfer

(34) Jandrasics, E. Z.; Keene, F. R. *J. Chem. Soc., Dalton Trans.* **1997**, 153.
(35) Glazer, E. C.; Tor, I. *Angew. Chem., Int. Ed.* **2002**, *41*, 4022.
(36) Demadis, K. D.; Hartshorn, C. M.; Meyer, T. J. *Chem. Rev.* **2001**, *101*, 2655 and references therein.

Table 4. Photophysical Properties[a]

	298 K			77 K	
complex	λ_{max} (nm)[b]	Φ	τ (ns)	λ_{max} (nm)	τ (ns)
$\mathbf{2}^{2+}$	994	3.5×10^{-4}	20	980	47
$\mathbf{3}^{2+}$	~1240	$<10^{-6}$	—[b]	~1240	—[b]
$\mathbf{4}^{4+}$	1110	7.5×10^{-5}	4	1096	16

[a] At the indicated temperature, in acetonitrile solvent; $\lambda_{exc} = 420$ nm (luminescence spectra) or 407 nm (luminescence lifetimes). Complexes $\mathbf{5}^{4+}$ and $\mathbf{6}^{4+}$ could not be measured because emission was too weak. [b] Too weak to measure.

mechanism, as opposed to a hole-transfer mechanism, as the higher-lying d_π orbitals of Os would allow more extensive mixing with the π^* orbital of the isoeilatin ligand because the energy gap between them is smaller.[4c] Previous measurements of the analogous dibenzoeilatin complexes, where the bridge has a larger fused aromatic surface, albeit distorted from planarity, exhibited similar ΔE values (0.16 and 0.25 V for the dinuclear Ru- and Os-dibenzoeilatin complexes, respectively).[11b] In general, the more extended the π-surface of a ligand, the greater the delocalization, and the greater the electronic communication enabled by the bridge, for a given metal-to-metal distance. (For both isoeilatin and dibenzoeilatin complexes, the distance is roughly the same − ca. 8 Å.) This is not the case here, which suggests that the distortion of dibenzoeilatin hinders, to some extent, the electronic communication between the metal centers.[37] The sequential one-electron oxidations produce mixed-valence species, the stability of which can be expressed in terms of the comproportionation constant, k_{com}.[4] The k_{com} values for the dinuclear complexes presented in Table 3 suggest moderate electronic coupling between the metal centers.

The heterodinuclear complex $\mathbf{6}^{4+}$ also exhibits two reversible metal-centered oxidations at 1.11 and 1.60 V vs SCE. The first oxidation process, corresponding to the $Os^{II/III}$ couple, is anodically shifted with respect to the first oxidation process observed for $\mathbf{5}^{4+}$, whereas the second oxidation process, corresponding to the $Ru^{II/III}$ couple, is slightly cathodically shifted with respect to the second oxidation process in $\mathbf{4}^{4+}$. Both observations reflect the greater electron-withdrawing capabilities of Ru and its diminished tendency to back-donate relative to Os.

Luminescence. The emission spectra of the complexes as the PF_6^- salts were recorded at room temperature in acetonitrile solution and at 77 K (in frozen solvent). Emission band maxima (λ_{max}), emission quantum yields (Φ), and lifetimes (τ) are listed in Table 4; luminescence spectra are displayed in Figure 7.

For both room-temperature and 77 K measurements, the luminescence spectral profiles are broad and exhibit a vibrational progression on the order of 1300 cm^{-1}, typical of ^{3}MLCT emitters.[38] The Ru(II) complex $\mathbf{2}^{2+}$ exhibits a room-temperature emission maximum at 994 nm, and coordination of a second Ru(II) metal leads to red-shifting

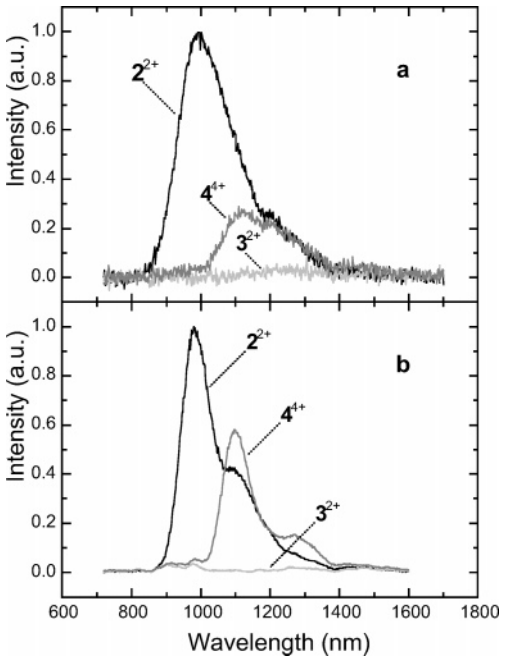

Figure 7. Luminescence spectra of isoabsorbing solutions ($\lambda_{exc} = 420$ nm) of the indicated complexes at (a) room temperature and (b) 77 K.

of the emission band maximum to 1110 nm. This is consistent with the stabilization of the π^* orbital of the isoeilatin ligand (which is involved in the ^{3}MLCT emission) by the coordination of a second metal center, as also observed in both the absorption spectra and the electrochemical measurements (vide supra). On passing from room temperature to 77 K, the emission levels of $\mathbf{2}^{2+}$ and $\mathbf{4}^{4+}$ exhibit a small blue shift (λ_{max} from 994 to 980 and from 1110 to 1096 nm, respectively). This behavior is consistent with the MLCT nature of the emissive state.[1a,1d,3,39−45] For the isoeilatin complexes, the emission level is shifted to very low energy, slightly lower than that observed for the related dibenzoeilatin complexes.[11b] (This is consistent with the electrochemistry results, indicating that isoeilatin is a better π-acceptor ligand, attributed to its less sterically hindered binding site and its planarity and despite its smaller fused aromatic surface; vide supra.) As a consequence, all of the Os(II)-containing complexes exhibit very weak emission intensities, and therefore, these complexes could not be investigated as luminophores; for $\mathbf{3}^{2+}$, $\mathbf{5}^{4+}$, and $\mathbf{6}^{4+}$, we estimate $\Phi < 10^{-6}$ at room temperature. This is likely due to expected effects from the energy gap law.[39−41] For

(37) It is also possible that differential association with the hexafluorophosphate counteranion might influence the redox behavior of the isoeilatin and dibenzoeilatin complexes. See: D'Alessandro, D. M.; Keene, F. R. *Dalton Trans.* **2004**, 3950.

(38) Elfring, W. H.; Crosby, G. A. *J. Am. Chem. Soc.* **1981**, *103*, 2683.

(39) Demadis, K. D.; Hartshorn, C. M.; Meyer, T. J. *Chem. Rev.* **2001**, *101*, 2655 and references therein.

(40) (a) Hammarström, L.; Barigelletti, F.; Flamigni, L.; Indelli, M. T.; Armaroli, N.; Calogero, G.; Guardigli, M.; Sour, A.; Collin, J. P.; Sauvage, J. P. *J. Phys. Chem. A* **1997**, *101*, 9061. (b) Treadway, J. A.; Loeb, B.; Lopez, R.; Anderson, P. A.; Keene, F. R.; Meyer, T. J. *Inorg. Chem.* **1996**, *35*, 2242. (c) Matacangay, A.; Zheng, G. Y.; Rillema, D. P.; Jackman, D. C.; Merkert, J. W. *Inorg. Chem.* **1996**, *35*, 6823.

(41) Englman, R.; Jortner, J. *Mol. Phys.* **1970**, *18*, 145.

(42) Caspar, J. V.; Kober, E. M.; Sullivan, B. P.; Meyer, T. J. *J. Am. Chem. Soc.* **1982**, *104*, 630.

(43) Barigelletti, F.; Flamigni, L.; Balzani, V.; Collin, J.-P.; Sauvage, J.-P.; Sour, A.; Constable, E. C.; Cargill-Thompson, A. M. W. *J. Am. Chem. Soc.* **1994**, *116*, 7692.

(44) Keene, F. R. *Coord. Chem. Rev.* **1997**, *166*, 121.

(45) Barigelletti, F.; Flamigni, L. *Chem. Soc. Rev.* **2000**, *29*, 1.

complex $\mathbf{3}^{2+}$, the estimated emission is substantially red-shifted with respect to the analogous Ru(II) complex $\mathbf{2}^{2+}$ (~1240 nm compared to 994 nm, respectively), consistent with the absorption spectra and the electrochemical measurements (vide supra). For the heterodinuclear complex $\mathbf{6}^{4+}$, no Ru-based emission was observed, which indicates that some quenching process occurs. The nature of this process could not be determined because of the lack of data concerning emission from the Os(II) complexes $\mathbf{3}^{2+}$ and $\mathbf{5}^{4+}$.

Conclusions

Isoeilatin, the third member of the eilatin family, is a conjugated ligand featuring two pyridyl-quinoline binding sites, that can be employed for the synthesis of mononuclear and homo- or heterodinuclear ruthenium and osmium complexes. In contrast to the other members of its family, isoeilatin remains planar after metal binding. Even though the surface area of isoeilatin is identical to that of eilatin, the dimerization tendency of its mononuclear complexes via π-stacking is significantly diminished. The electrochemical and photophysical properties of its complexes are closely related to those of the other members of the eilatin family, signifying that the substitution pattern around the tetraazaperylene core and the deviation from planarity have little effect on the energies of the frontier orbitals.

Acknowledgment. This research was supported by the Israel Science Foundation founded by the Israel Academy of Sciences and Humanities and by FIRB Project RBNE019H9K "Molecular Manipulation for Nanometric Devices" of MIUR. We thank Mrs. Dvora Reshef (TAU) for technical assistance and Dr. Francesco Barigelletti (ISOF-CNR) for valuable discussions.

Supporting Information Available: Stereoviews of the packing of **1**·$[HCl]_2$ and *meso*-**4**·$[Cl]_4$ and ORTEP view of *meso*-**5**·$[PF_6]_4$; X-ray crystallographic file in CIF format for the structure determinations of **1**·$[HCl]_2$ and of the complexes *meso*-**4**·$[PF_6]_4$, *meso*-**4**·$[Cl]_4$, and *meso*-**5**·$[PF_6]_4$. This material is available free of charge via the Internet at http://pubs.acs.org.

IC050002Q